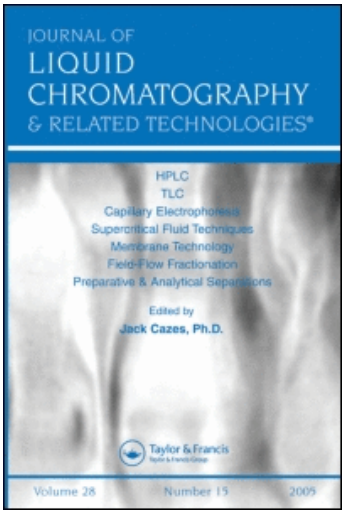

Journal of Liquid Chromatography & Related Technologies
Publication details, including instructions for authors and subscription information:
http://www.informaworld.com/smpp/title~content=t713597273

Comparison of Retention Behavior of Various Polystyrene Latex Particles and Gold Colloids on Different Channel Walls in Flow Field-Flow Fractionation

Jong Hee Song[a]; Won-Suk Kim[b]; Dai Woon Lee[a]
[a] Department of Chemistry, Yonsei University, Seoul, Korea [b] Department of Chemistry and the Beckman Institute, University of Illinois, Urbana-Champaign, Illinois, USA

Online publication date: 10 September 2003

To cite this Article Song, Jong Hee , Kim, Won-Suk and Lee, Dai Woon(2003) 'Comparison of Retention Behavior of Various Polystyrene Latex Particles and Gold Colloids on Different Channel Walls in Flow Field-Flow Fractionation', Journal of Liquid Chromatography & Related Technologies, 26: 18, 3003 — 3035
To link to this Article: DOI: 10.1081/JLC-120025416
URL: http://dx.doi.org/10.1081/JLC-120025416

JOURNAL OF LIQUID CHROMATOGRAPHY & RELATED TECHNOLOGIES®
Vol. 26, No. 18, pp. 3003–3035, 2003

Comparison of Retention Behavior of Various Polystyrene Latex Particles and Gold Colloids on Different Channel Walls in Flow Field-Flow Fractionation

Jong Hee Song,[1] Won-Suk Kim,[2] and Dai Woon Lee[1,*]

[1]Department of Chemistry, Yonsei University, Seoul, Korea
[2]Department of Chemistry and the Beckman Institute, University of Illinois, Urbana-Champaign, Illinois, USA

ABSTRACT

Flow field-flow fractionation (FlFFF) is a high-resolution technique for separating and characterizing particulate materials into well-defined particle fractions by size in the approximate diameter range 1–100 μm. Retention of the sample particle is affected by the property of the accumulation wall, which is composed of a polymer membrane. In this work, retention behavior of three polystyrene latex spheres (having diameters of 50, 105, and 152 nm), high and low charged synthetic polymeric particles (having diameters of 115 and 180 nm), and 5, 10, 20 nm-sized gold colloid standards are studied on two different types of membranes; a hydrophilic regenerated cellulose membrane and a hydrophobic polysulfone membrane. Both membranes have the same molecular

*Correspondence: Dai Woon Lee, Department of Chemistry, Yonsei University, 134 Shinchondong Seodaimoongu, Seoul 120-749, Korea; E-mail: leedw@yonsei.ac.kr.

DOI: 10.1081/JLC-120025416
1082-6076 (Print); 1520-572X (Online)

MARCEL DEKKER, INC.
270 Madison Avenue, New York, New York 10016

weight cutoff of 10 kDa. Retention was measured for each sample at various pH and ionic strength of the carrier liquid. Several kinds of surfactants were also tested.

Key Words: Nano; Flow field fractionation; Colloid; Membrane; Gold; Particle-wall interaction; Polysulfone; Regenerated cellulose.

INTRODUCTION

Various kinds of polymers can be used as a barrier of the membrane material, but the chemical and physical properties differ so much that only a limited number will be used in practice. The properties of the membrane materials are completely determined by the presence of the ionic groups. Due to a high affinity to water, such polymer swells quite strongly in aqueous solutions or even becomes soluble. For the microfiltration/ultrafiltration membranes, the choice of the material is mainly determined by the processing requirement (membrane manufacture), fouling tendency, and chemical and thermal stability of the membrane.[1–3]

In the cross-flow operation, the feed flows parallel to the membrane surface with the inlet feed stream entering the membrane module at a certain composition. Flux decline is relatively smaller with cross-flow and can be controlled and adjusted by proper module choice and cross-flow velocities. To reduce concentration polarization and fouling as much as possible, the membrane process is generally operated in a cross-flow mode. The cross-flow velocity is the main parameter that determines mass transfer in the module. Because of the merits of the cross flow module, it can be applied to the analytical instruments.

The membrane accumulation wall is the heart of the flow field-flow fractionation (FlFFF) channel. Desirable membrane properties include smoothness, uniform pore size, and distribution, compatibility with the carrier liquids, and minimal interactions with sample species. Recovery of sample species is the determining factor in identifying a suitable membrane for application to the easily adsorbed materials. The degree of such interaction depends on various parameters including the surface properties of the sample, suspending medium, surface potential of the membrane, temperature, ionic strength of the carrier liquid,[4,5] etc. In this work, a comparison of recovery and resolution can be used for interpretation[6] of the difference between the regenerated cellulose membrane and polysulfone membrane. Many researchers already have investigated the particle–wall interaction in sedimentation field-flow fractionation (FFF), but the study of particle–wall interaction in the

MARCEL DEKKER, INC.
270 Madison Avenue, New York, New York 10016

flow FFF has not been as successful because of difficulty in the adjustment of flow rate and field strength.[7–9]

We investigated the retention behavior for the purpose of optimization and choice of the proper experimental conditions at given accumulation wall materials and carrier solutions in the flow FFF system. One of the main causes of departure from the FFF theory is the interaction between the sample and the accumulation wall. During elution, particles are driven towards equilibrium positions between the channel walls where the force due to the applied field is balanced by a hydrodynamic lift force. The elution of polystyrene latex particles under various field strength and carrier flow rate yields information on lift force as a function of particle size, flow velocity, position within the channel, and any other controllable system property.[10,11]

From the observed change in retention, the interaction between the sample particle and the membranes can be calculated. The experimental data were used to compare the properties of different types of membranes, hydrophilic regenerated cellulose membrane, and hydrophobic polysulfone membrane.

EXPERIMENTAL

Instrumentation

The flow field-flow fractionation system used in this study is the model F-1000 Universal Fractionator from FFFractionation, LLC (Salt Lake City, UT). The channel outline was cut from a Mylar strip 254 μm thick, and had a breadth b of approximately 2 cm and a tip-to-tip length L_{tt} of 29.7 cm. The Mylar strip was used as a spacer between the two parallel channel walls. The void volume of the channel was determined to be 1.28 mL by calibration with the polystyrene latex standards.

The carrier solution was pumped by an Eldex Metering CC-100-S-4 pump (Eldex Laboratories, Inc., Napa, CA). The eluted particles were monitored by a M720 UV-VIS detector (Young-In Scientific Co., Seoul, Korea) operating at the fixed wavelength of 254 nm for polystyrene latex particles. The detector signal was processed using FFF software obtained from FFFractionation, LLC. Samples were injected using a Model 7125 loop injector (Rheodyne, Inc., Cotati, CA). The injection volume was 10 μL depending on the sample concentration. Flow FFF systems are generally constructed with a compressible membrane used for the accumulation wall. For a comparison of retention behavior on different channel walls in flow FFF, two different kinds of membranes were used for the channel accumulation wall. One is the hydrophilic regenerated cellulose membrane and the other is the hydrophobic polysulfone membrane. All of the membranes have the same pore size of

Marcel Dekker, Inc.
270 Madison Avenue, New York, New York 10016

MWCO 10 kDa from FFFractionation, LLC (Salt Lake City, UT). The zeta potential of polystyrene latex particles was measured by the Zeta Potential Analyzer (Dynamic Laser Light Scattering Zeta Plus, Brookhaven Instruments Co., USA).[12–14]

Chemicals and Reagents

Carrier solutions were made using doubly distilled deionized water. For the calibration of the system, 0.1% (w/v) solution of Fl-70 detergent from Fisher Scientific (Fairlawn, NJ) with 0.02% sodium azide added as a bactericide was used. This carrier composition is commonly used for latex size analysis by FFF. Fl-70 is composed of 3.0% oleic acid, 3.0% sodium carbonate, 1.8% Tergitol, 1.4% tetrasodium EDTA, 1.3% triethanolamine, and 1.0% polyethylene glycol, made up in water. Nonionic surfactant Triton X-100 (9-10 ethoxyoctylphenol) is miscible with water, alcohol, and acetone. Cetyltrimethyl ammonium bromide (CTAB) was used for cationic surfactant. The last two surfactants were purchased from Sigma Aldrich, Inc. (St. Louis, MO). Figure 1 shows the structures of surfactant molecules. The carrier solution for pH studies is Triton X-100 with 0.02% sodium azide, and sodium hydroxide and phosphoric acid was added for adjusting of pH. The particles used in this research were polystyrene-divinyl benzene copolymer latex standards of nominal diameter 50, 105, 152 nm samples (Duke Scientific, Palo Alto, CA) and 5, 10, 20 nm-sized gold colloid standards (Sigma Aldrich, Inc., St. Louis, MO). They are listed in Tables 1 and 2. The charged polymer particles were synthesized with different surface charge density by emulsifier-free emulsion polymerization. The surface charge

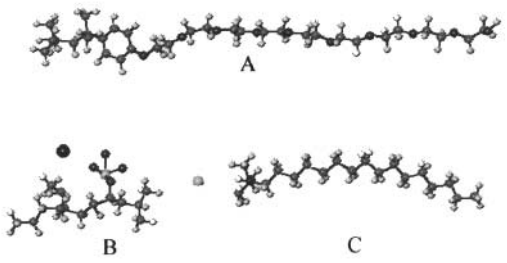

Figure 1. Molecular structures of (A) Triton X-100, (B) Tergitol, (C) CTAB. These structures are described by Hyperchem 7.

MARCEL DEKKER, INC.
270 Madison Avenue, New York, New York 10016

Table 1. Polystyrene latex particles used in this work.

Polystyrene latex	Nominal diameter (nm)	Surface charge density ($\mu C/cm^2$)	Source
Polystyrene latex standards	50 105 152	22	Duke Scientific
High charge density polystyrene latex	115 180	56	Synthesized
Low charge density polystyrene latex	115 180	6.1	Synthesized

density was measured by conductometric titration after the latexes had been rigorously cleaned.

RESULTS AND DISCUSSION

Polystyrene latex particles were used for the probe of particle–wall interaction at different type of accumulation wall and carrier fluid composition. The surface property of polystyrene latex particles has a different effect on the adsorption behavior. In this study, two kinds of polystyrene latex particles with different surface charge density were prepared. They were synthesized through emulsifier-free emulsion polymerization and their surface charge density was 6.1 and 56 $\mu C/cm^2$, respectively. Polystyrene latex particles with high charge density means they have a greater number of anionic charge groups on their surface that can be related to the electrostatic repulsion with the anionic group. From the comparison of the recovery of each sample, it

Table 2. Gold colloid standards used in this work.

Nominal size (nm)	Measured diameter by flow FFF system (nm)	Source
5	7.5	Sigma Aldrich
10	16.6	Sigma Aldrich
20	29.6	Sigma Aldrich

Marcel Dekker, Inc.
270 Madison Avenue, New York, New York 10016

is assumed that negatively charged particles keep more repulsion force between accumulation wall and particle surface. Numerical calculations of particle–wall interaction based on the DLVO theory, and their effect on particle concentration profiles and retention ratios, have been reported.[15,16]

The classical Derjaguin–Landau–Verwey–Overbeek theory takes into account electric diffuse double-layer repulsion and London–van der Waals attraction; a potential barrier that a particle must surmount in order to collide and unite with a second particle is dependent on electrolyte concentration and counterion valence in a manner capable of explaining the interaction energy quantitatively. Calculation of the energy of repulsion between spherical particles can be carried out by this famous formula.[17–21]

$$V_R = 16\varepsilon\varepsilon_0 r_p \psi_1 \psi_2 \left(\frac{kT}{Ze_0}\right)^2 \times \ln(1 + \exp(-\kappa H)) \tag{1}$$

$$\psi_i = \tanh\left(\frac{Ze_0\phi_i}{kT}\right) \tag{2}$$

$$\kappa^2 = \frac{2{e_0}^2 N_A I}{\varepsilon\varepsilon_0 kT} \tag{3}$$

ε is the dielectric constant, ε_0 is the permittivity of the vacuum, Z is the valence of the ion, e_0 is the electron charge, r_p is the particle radius, ϕ_i is the surface potential, κ is the reciprocal double-layer thickness, k is the Boltzmann constant, N_A is Avagadro's constant, I is the ionic strength, T is the temperature and H is the distance of the sphere from the surface. This integration can equally well be applied to the exact numerical results for flat plates, and to the constant charge case as well as to the constant potential case. When $\exp(-\kappa H)$ is small, logarithmic term using the relation of $\ln(1+x) = x$,

$$V_R = 16\varepsilon\varepsilon_0 r_p \psi_1 \psi_2 \left(\frac{kT}{Ze_0}\right)^2 \times \ln(1 + \exp(-\kappa H)) \approx C\ \exp(-\kappa H) \tag{4}$$

As the particle approaches the surface, the potential energy due to the van der Waals attractive force for particle–wall interaction can be calculated from

$$V_A = \frac{A_{132}}{6}\left(\frac{r_p}{H} + \frac{r_p}{H + 2r_p} + \ln\left(\frac{H}{H + 2r_p}\right)\right) \tag{5}$$

Subscripts 1 and 2 refer, respectively, to the particle and wall material and subscript 3 represents the medium. A_{132} is the Hamaker constant. The range of operation of the van der Waals force may be estimated by comparing the

MARCEL DEKKER, INC.
270 Madison Avenue, New York, New York 10016

thermal energy with V_A. Values of Hamaker constant A are in the range of 10^{-20} to 10^{-19} J. Thus, for two dissimilar materials, Hamaker constant is

$$A_{12} \approx \sqrt{A_{11}A_{22}} \tag{6}$$

For contact of two dissimilar materials in the presence of the third media:

$$A_{132} \cong \left(\sqrt{A_{11}} - \sqrt{A_{33}}\right)\left(\sqrt{A_{22}} - \sqrt{A_{33}}\right) \tag{7}$$

The total interaction is:

$$V_T = C\ \exp(-\kappa H) - \frac{A_{132}r_p}{6}\left(\frac{r_p}{H} + \frac{r_p}{H+2r_p} + \ln\left(\frac{H}{H+2r_p}\right)\right) \tag{8}$$

A_{132} depends on the dispersion medium. The Hamaker constant of water and several aliphatic alcohols in free space are reported to have similar values, on the order of 10^{-20} J. Total interaction energies are calculated as a function of the particle–wall distance at different ionic strengths. At low ionic strengths, the electrical double layer is relatively thick compared to r_p, so the long-range repulsive force prevents the particles from getting close to each other. However, by increasing the ionic strength, the surface charges are shielded, permitting closer contact. This leads to attraction between the surfaces. The sum of the different interaction energies depend, additionally, upon a variety of properties of the particles, the suspending medium, and the channel wall. The reduced repulsive effects caused by an increased level of ionic shielding allow attractive forces to become more dominant. As the repulsive barrier drops lower as a consequence of gain in ionic strength, an increasing number of colloidal particles will cross the barrier and, thus adhere to the wall, giving rise to a probable loss of sample and a fouling of the channel surface. Such losses are highly undesirable for practical operation.[22]

One of the possibilities to minimize the particle–particle and particle–wall interactions, is consequently to choose the proper ionic strength so the total interaction energy as close to zero as possible. Another possibility to alter the interaction energy is to add a surfactant. Surfactant molecules adsorb to the particle surface and stabilize the particles by a steric hindrance and repulsive charge.

All constants needed for the calculations are shown in surface potential of polystyrene latex particle is $\phi_1 = -80$ mV, regenerated cellulose membrane is $\phi_2 = -20$ mV and polysulfone membrane is $\phi_2 = -8$ mV independent of I. All

Table 3. Collection of parameters used in the calculation of particle–wall interaction energies.

Materials	Hamaker constant ($\times 10^{-20}$ J)	Surface potential (mV)	References
Polystyrene latex	7.9	−80	[23]
Gold	40	−30	[24,25]
Water	4	—	[26]
Cellulose	8.6	−20	[27]
Polysulfone	7	−8	[28,29]
Cellulose-water-PS latex	0.76	—	Calculated
Cellulose-water-PS latex	4.03	—	Calculated
Polysulfone-water-PS latex	0.52	—	Calculated
Polysulfone-water-PS latex	2.79	—	Calculated

of values used in the calculation of particle–wall interaction energy in aqueous solutions are summarized in Table 3.[23–29]

Figure 2 shows that the potential energy profile (expressed in terms of J at 298 K) for the 100 nm sized polystyrene latex on the different membrane surface. The value of repulsion potential energy of the polystyrene latex on polysulfone membrane is smaller than that of regenerated cellulose membrane because of the lower surface potential of the former. As the ionic strength increases, the repulsive maxima become smaller and narrower. Figure 3 shows that the potential energy profile for the different sized polystyrene latex on regenerated cellulose membrane. The dashed line is the double layer thickness at that condition. Figure 4 shows that the potential energy profile for the 20 nm sized gold colloid on the different membrane surface. The value of repulsion potential energy of the gold colloid on polysulfone membrane is smaller than that of regenerated cellulose membrane because of the lower surface potential of the former. The potential energy is diminished at various ionic strength conditions compared to that of polystyrene latex particles because of the larger value of the Hamaker constant. Figure 5 shows the potential energy profile for the different sized gold colloids on regenerated cellulose membranes.

Particle–wall interaction was predicted to result in an increment to R, meaning good approximation. This was supported by our experimental results. Figure 6 shows the zeta potential of high and low charge density particles in various carrier solutions. Except for the cationic detergent CTAB, all of the polystyrene latex particles have the negative zeta potential that may cause the repulsion force between each particle in applied carrier conditions.

MARCEL DEKKER, INC.
270 Madison Avenue, New York, New York 10016

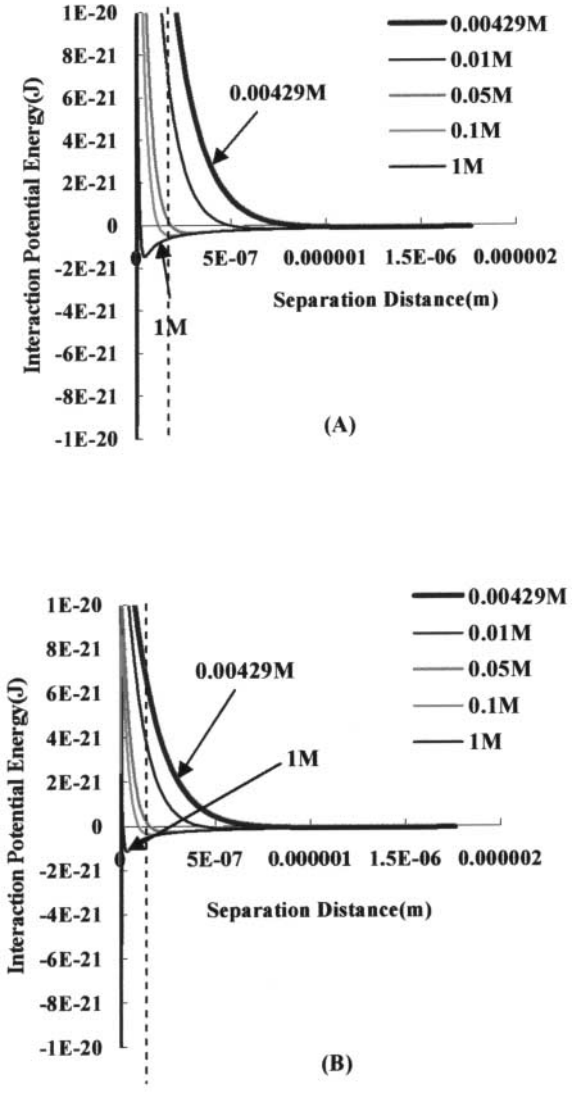

Figure 2. Calculated interaction potential energy (expressed in terms of J at 298 K) for the 100 nm sized polystyrene latex on regenerated cellulose membrane (A) and polysulfone membrane (B) at various ionic strength of carrier solution.

MARCEL DEKKER, INC.
270 Madison Avenue, New York, New York 10016

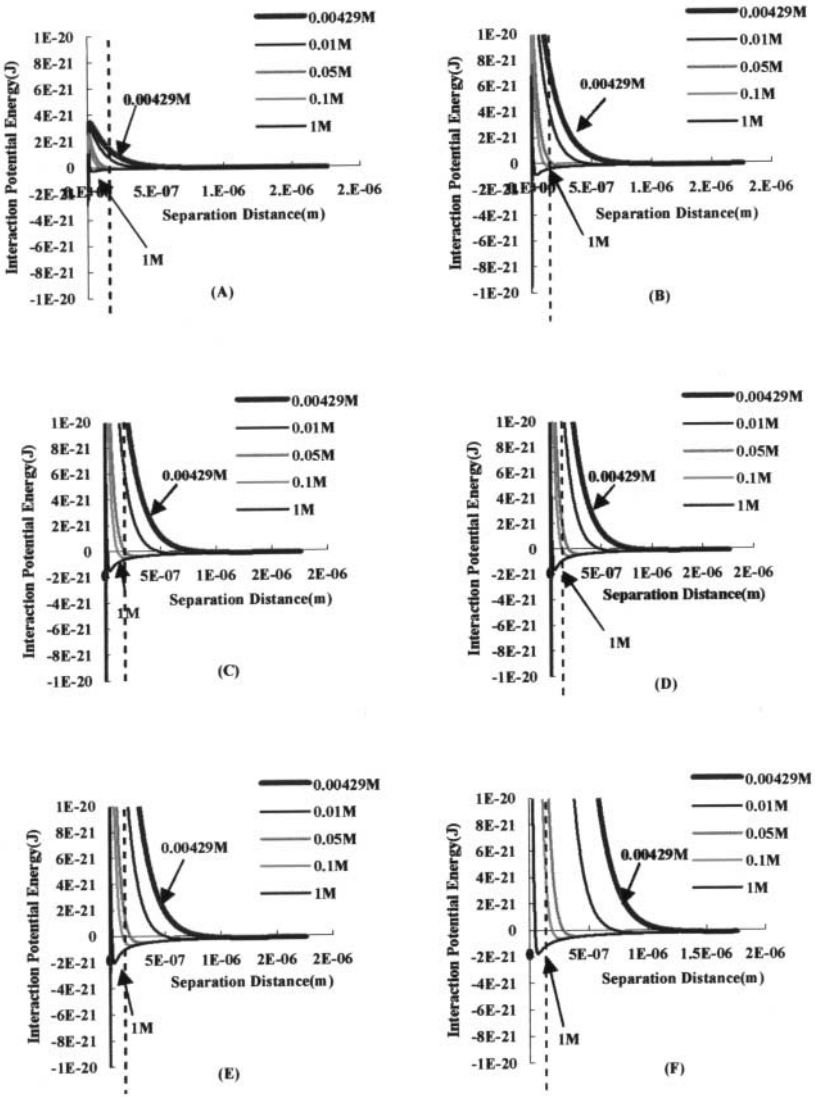

Figure 3. Calculated interaction potential energy (expressed in terms of J at 298 K) for the 10 nm (A), 50 nm (B), 100 nm (C), 115 nm (D), 150 nm (E), and 180 nm (F) sized polystyrene latex on regenerated cellulose membrane.

MARCEL DEKKER, INC.
270 Madison Avenue, New York, New York 10016

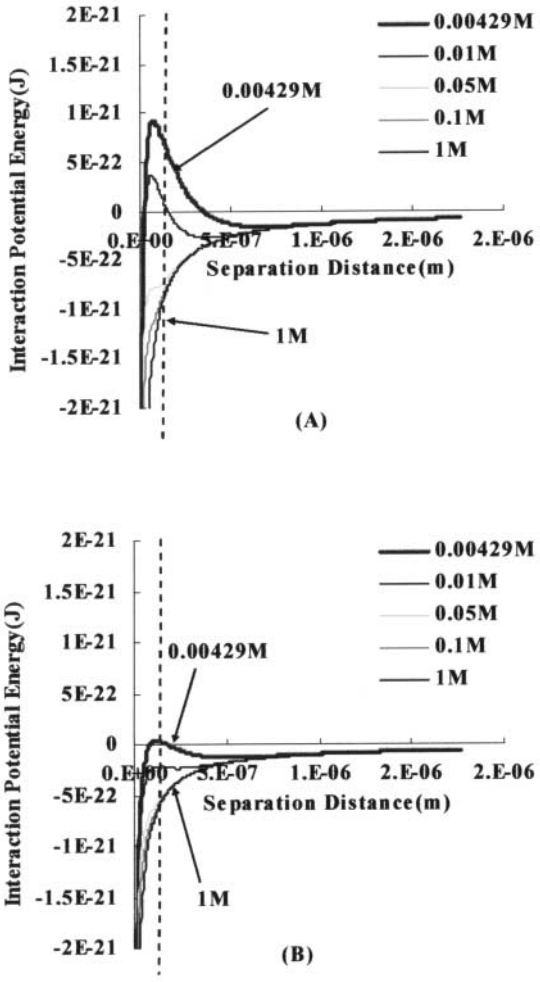

Figure 4. Calculated interaction potential energy (expressed in terms of J at 298 K) for the 20 nm sized gold colloid on regenerated cellulose membrane (A) and polysulfone membrane (B) at various ionic strength of carrier solution.

As the adsorbent species and the adsorbate are similarly charged, the tendency of repulsion is similar in several applied carrier solutions, except for the CTAB. The abnormal experimental trend is probably due to changes in the concentration profile near the wall. It is important to discuss first the surface charge interactions and propose if the surfactant added carrier is needed for proper separation in flow FFF.

Marcel Dekker, Inc.
270 Madison Avenue, New York, New York 10016

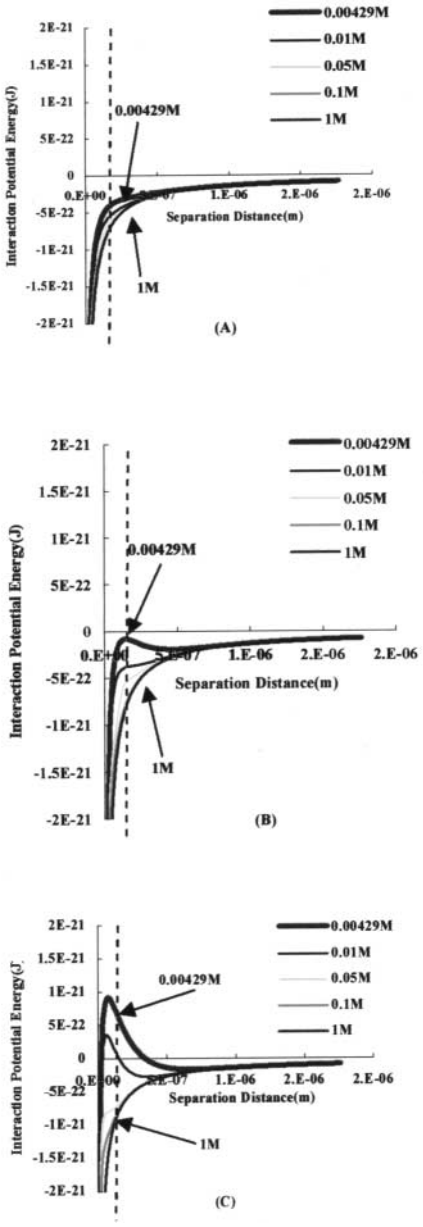

Figure 5. Calculated interaction potential energy (expressed in terms of J at 298 K) for the 5 nm (A), 10 nm (B), and 20 nm (C) sized gold colloid on regenerated cellulose membrane.

MARCEL DEKKER, INC.
270 Madison Avenue, New York, New York 10016

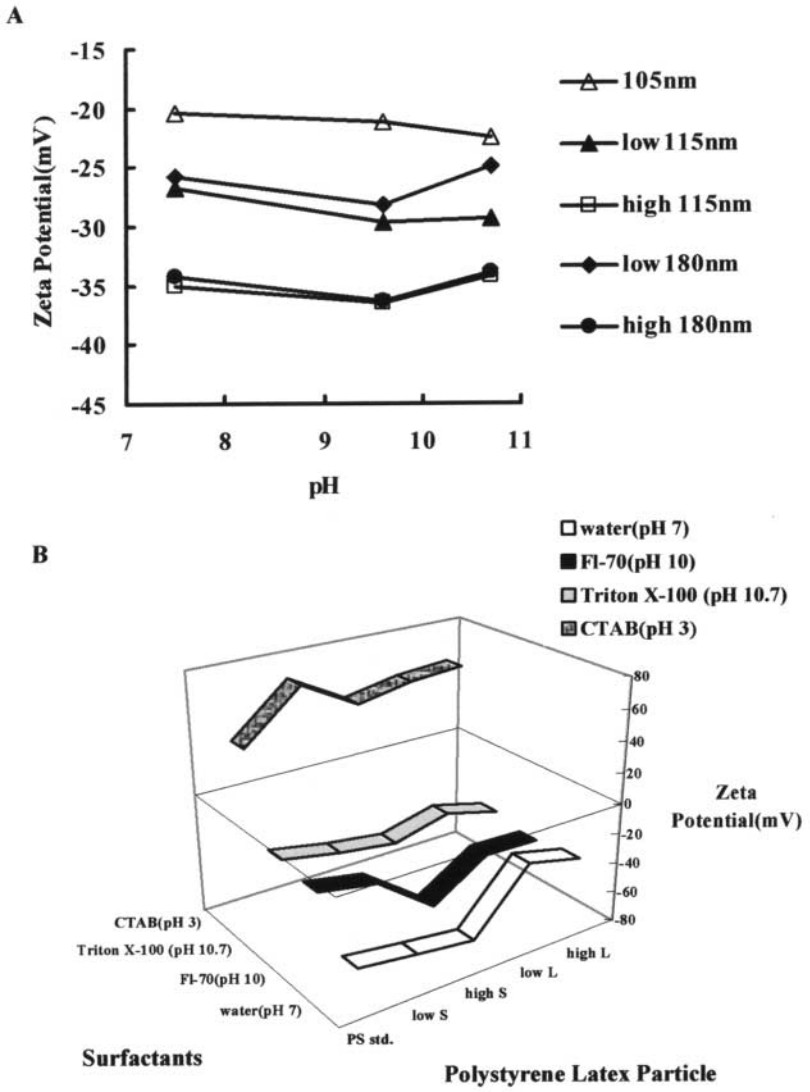

Figure 6. (A) Zeta potential of polystyrene latex particles at different pH conditions, carrier solutions are 0.1% Triton X-100 added sodium hydroxide and phosphoric acid for adjustment of pH. (B) Zeta potential of polystyrene latex particles at different surfactant conditions. PS std. is 105 nm sized polystyrene latex standard particle, low S is 115 nm sized low charge density polystyrene latex, high S is 115 nm sized high charge density polystyrene latex, low L is 180 nm sized low charge density polystyrene latex and high L is 180 nm sized high charge density polystyrene latex.

MARCEL DEKKER, INC.
270 Madison Avenue, New York, New York 10016

Effect of Ionic Strength of Carrier Solution

Flow FFF measurements are shown at several series of carrier solutions on two different types of membranes. One is the hydrophilic regenerated cellulose membrane and the hydrophobic polysulfone membrane. At low ionic strength, the particle zone was measurably repelled out of the sluggish flow region near the wall and eluted earlier than predicted. The concentration profiles in solutions of high ionic strength were enriched in the area of net attractive potential close to the wall and were excessively retained.

Several forces are active when a particle approaches a wall. The static forces include the van der Waals and electrostatic repulsive forces. Also, Born repulsion and solvent restructuring forces may create some aberrant results within a short distance from the wall. Additionally, hydrodynamic forces due to shear force near the wall will be important for larger particles at high flow rates. For polyelectrolytes, the repulsion will extend only a few times the double layer thickness into the solution, leading to a thin region from which polymers will be excluded of typical dimensions from 1 to 50 nm, depending on the ionic strength.[22] The adsorption of a monolayer of sample material onto the membrane will have an effect on retention, which can, in most cases, be further reduced by increases in ionic strength.

Ideally, there should be no adsorption, even in the presence of strong interactions. And the polymer adsorption should be self-limiting because of the electrostatic and steric repulsion effects. At worst, a few micrograms of polymer would be needed for the conditioning of the surface.[30] In aqueous media, surfactant adsorption can alter the dispersion properties by changing the van der Waals attraction, electrostatic repulsion, and steric forces between the particles.

After the adsorption of a certain amount of Triton X-100 molecules on the membrane surface and the particle surface, hydrogen bonding is proposed to be the initial driving force for interactions of the ethoxyoctyl chains with the hydroxylated surface. With the increase of the surface charge due to adsorption of the surfactant, particularly above the specific concentration, the solution composition had little effect on the retention. Also, the surface is shown to be hydrophilic.[31] An increase of the ionic strength of the carrier solution causes a decrease of the electric double layer thickness, particularly above the specific concentration; we found not only the increment of the retention but also the broadening of particle peak.

At the low ionic strength, a certain amount of repulsion force remains between the sample particles and membrane due to the balance of counterions in the diffuse layer. But at the higher ionic strength, ions bound by strong Coulomb attraction and short-range attraction build up the so-called Stern layer.[32,33] Regarding the effective surface charge density of the membrane on the basis of the effects of ion-pair formation between the membrane and

MARCEL DEKKER, INC.
270 Madison Avenue, New York, New York 10016

counterions, the swelling tendency and the effect of membrane pore size have been considered. Some of the charged groups within membranes with hydrophobic matrix polymers cannot be hydrated because they are less accessible to water molecules. In these cases, hydrophobic membranes are more likely to form ion pairs with counterions than hydrophilic membranes, thus leading to a suppression of dissociation of the charge groups. Also hydrophilic membranes are highly hydrated, therefore, their local dielectric constants might be high enough for ion-pairing effects to decay. It was predicted that repulsive effects near the wall would dominate experiments conducted in low ionic strength solutions, with a consequent increase in *R* values. At higher ionic strengths, the attractive forces play an important role, eventually leading to a decrease in the *R* values. These conclusions agree fully with the results of the various ionic strengths of carrier solutions shown in Figs. 7 and 8.

Effect of pH of Carrier Solution

When a certain amount of surfactant was added to the carrier solution, the retention times were not changed significantly at various pH ranges, but the intensity of peaks is decreased at an acidic condition. Actually, the pH of the carrier solution should affect the tendency of surface charge interaction due to the proton transfer.[34] Figure 9 shows the calculated hydrodynamic diameter at various pH of the carrier solution on two different membranes. At a lower pH condition, the recovery of polystyrene latex particles is reduced, unlike that of a higher pH condition, and retention time also tends to increase. Moreover, resolution of each peak on the polysulfone membrane is reduced, unlike that on the regenerated cellulose membrane.

Effect of Temperature

Figure 10 shows the retention behavior of polystyrene latex particles at different temperature conditions on both membranes. As the polystyrene latex particles are also polymer material, the surface property of the sample particle was further influenced by physical stress like temperature conditions. In fact, the increment of retention times of the polystyrene latex particles on the polysulfone membrane was smaller than that of the regenerated cellulose membrane.

Marcel Dekker, Inc.
270 Madison Avenue, New York, New York 10016

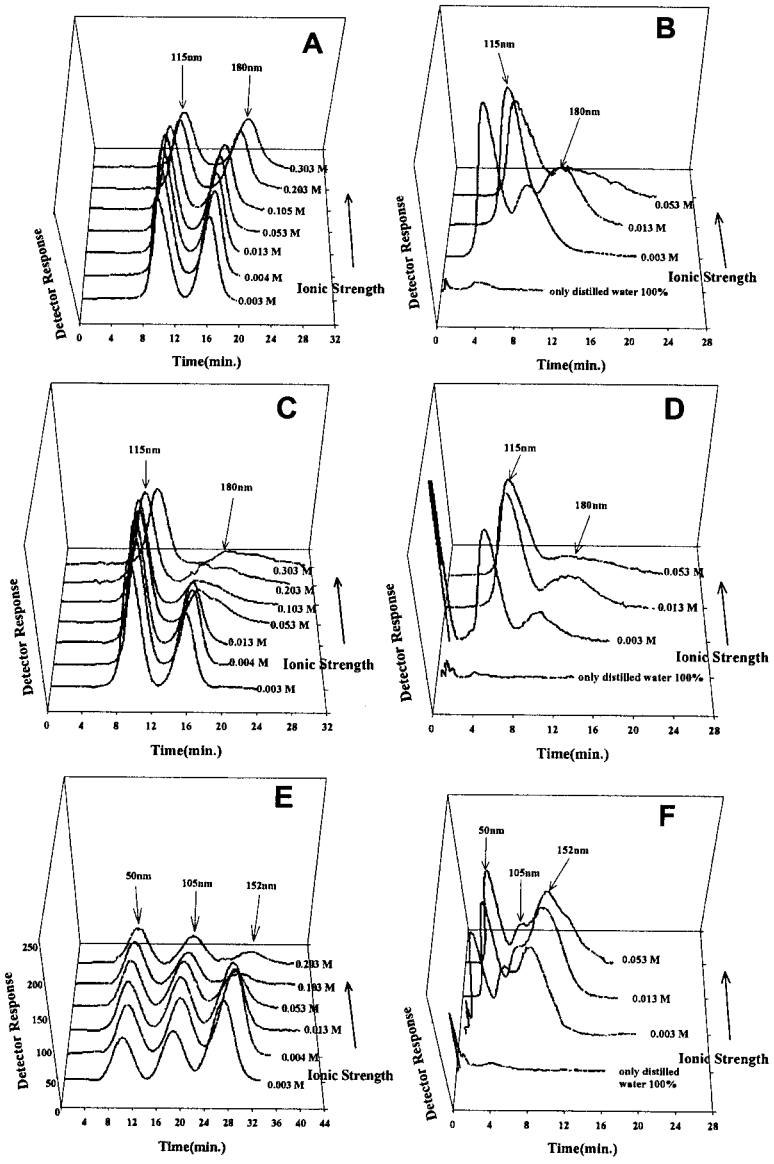

Figure 7. Fractograms of (A) high charged 115, 180 nm PS latex, (C) low charged 115, 180 nm PS latex, (E) 50, 105, 152 nm PS latex standards on regenerated cellulose membrane and (B) high charged 115, 180 nm PS latex, (D) low charged 115, 180 nm PS latex, (F) 50, 105, 152 nm PS latex standards on polysulfone membrane carrier solution is 0.1% Triton X-100 added with 0.02% NaN_3 and NaCl.

MARCEL DEKKER, INC.
270 Madison Avenue, New York, New York 10016

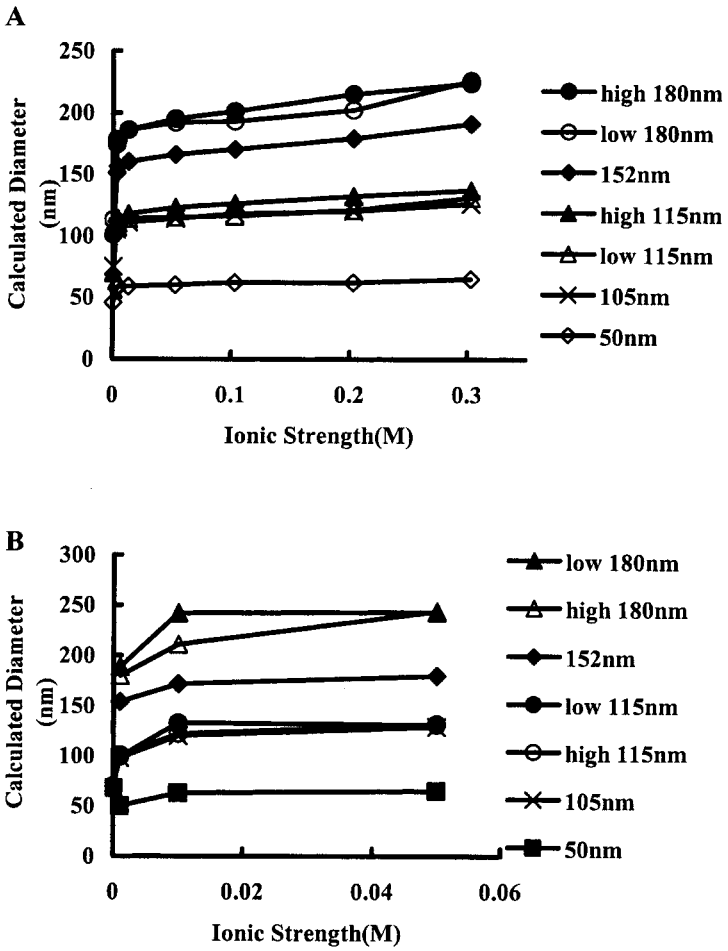

Figure 8. Calculated hydrodynamic diameter of 50, 105, 152 nm PS latex standards and high & low charged 115, 180 nm PS latex on regenerated cellulose (A) and on polysulfone membrane (B) at various ionic strength. Carrier solution is 0.1% Triton X-100 added with 0.02% NaN_3 and NaCl. Channel/cross flow rates are 2.2/0.7 mL/min.

Effect of Carrier Solution at Different Field Strengths

The departure of retention times of polystyrene latex particles on the polysulfone membrane, at different kinds of surfactant used for the carrier solution, is significantly greater than that on the regenerated cellulose membrane. These results indicated the difference of swelling property and

MARCEL DEKKER, INC.
270 Madison Avenue, New York, New York 10016

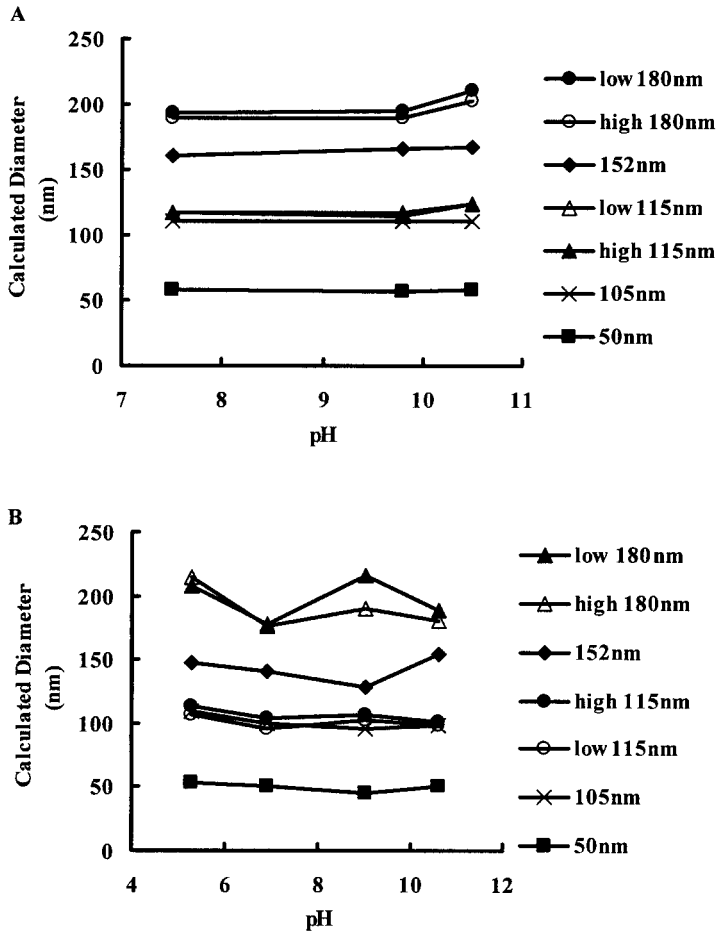

Figure 9. Calculated hydrodynamic diameter of polystyrene latex 50, 105, 152 nm and high & low charged 115, 180 nm polystyrene latex particles on regenerated cellulose membrane (A) and on polysulfone membrane (B) at various pH conditions. Carrier solution is 0.1% Triton X-100 added with 0.02% NaN_3 and NaOH or H_3PO_4. Channel/cross flow rates are 2.2/0.7 mL/min.

the surface charge difference of each membrane indirectly. Triton X-100 is the nonionic surfactant that is a little bit hard to adsorb on the surface of the hydrophobic polysulfone membrane, because it has no charged groups on its molecules. Moreover, it has the bulky side groups. It may cause the steric exclusion near the membrane surface. On the other hand, Fl-70 is widely used

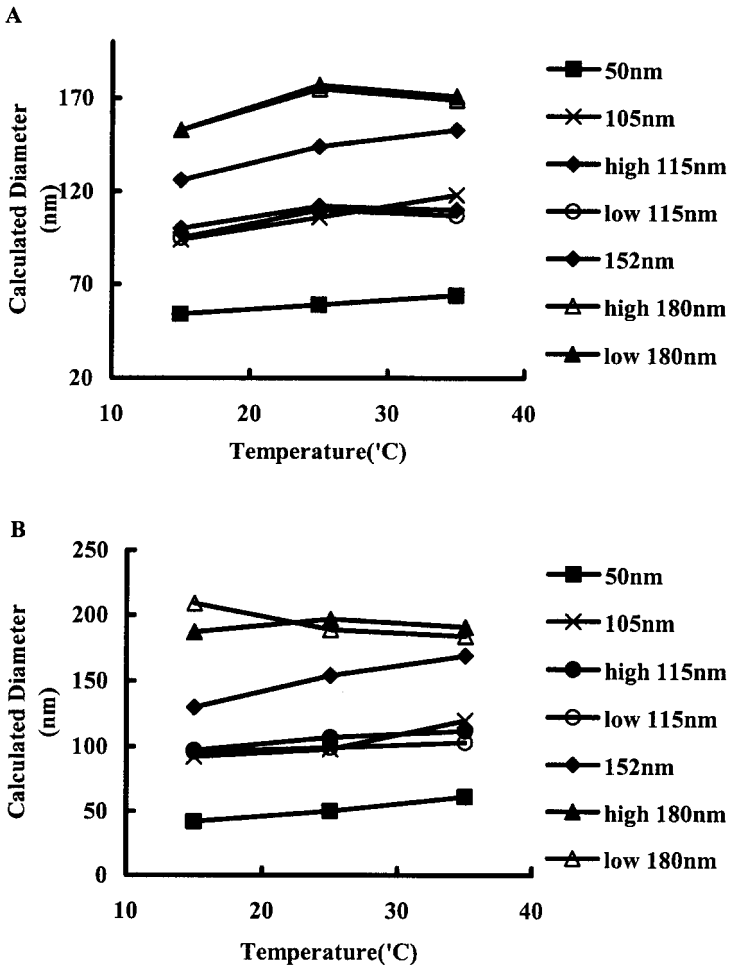

Figure 10. Calculated hydrodynamic diameter of polystyrene latex 50, 105, 152 nm and high & low charged 115, 180 nm polystyrene latex at different temperature on regenerated cellulose membrane (A) and on polysulfone membrane (B). Carrier is 0.1% Triton X-100 added with 0.2% sodium azide. Channel/cross flow rates are 2.2/0.7 mL/min.

for the carrier solution in FFF. The main component of Fl-70 is Tergitol, 7-ethyl-2-methyl-4-undecyl sulfate sodium salt. Because of the center position of its ionic sulfate residue, its wetting and penetration property is enhanced more than that of any other surfactant. It also has no benzene rings in its molecules. Tergitol is widely used as a penetration reagent because of these reasons.

MARCEL DEKKER, INC.
270 Madison Avenue, New York, New York 10016

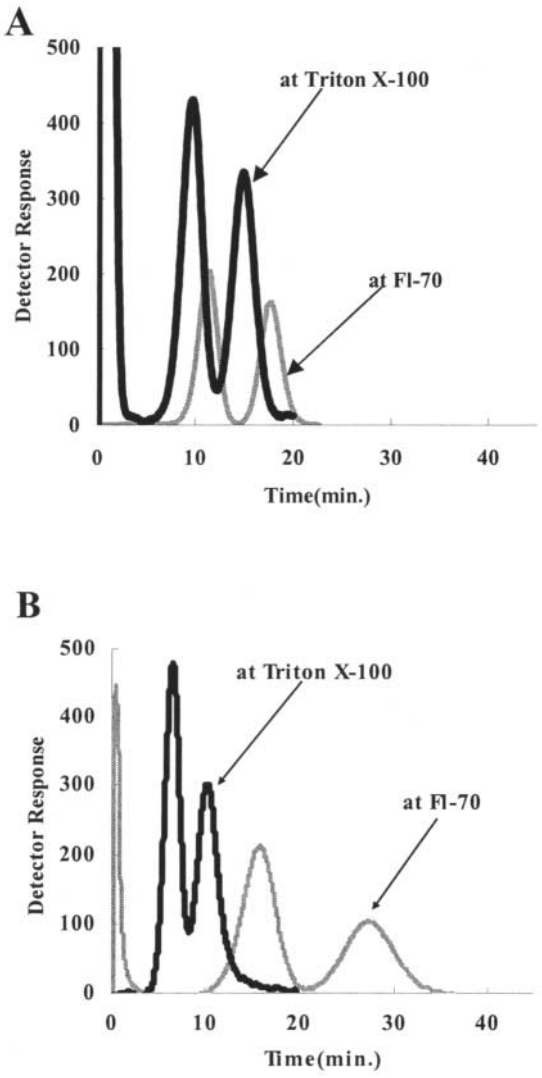

Figure 11. Fractograms of (A) high charged PS latex 115, 180 nm particles, on regenerated cellulose membrane and (B) high charged PS latex 115, 180 nm particles on polysulfone membrane at different carrier solutions. Channel/cross flow rates are 2.2/0.7 mL/min. Each surfactant concentrations are 0.1% added with 0.02% sodium azide.

MARCEL DEKKER, INC.
270 Madison Avenue, New York, New York 10016

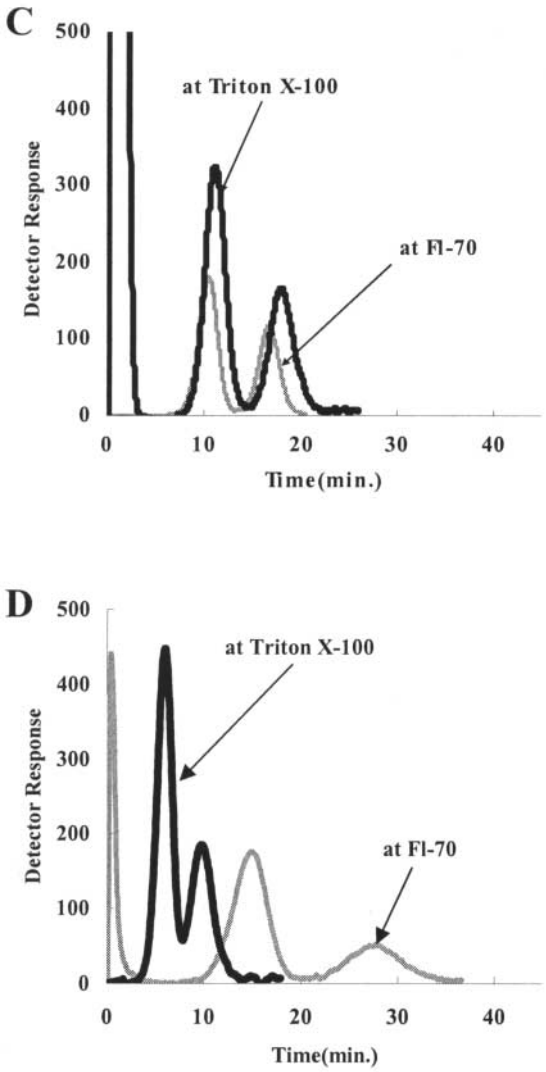

Figure 12. Fractograms of (C) low charged PS latex 115, 180 nm particles on regenerated cellulose membrane and (D) low charged PS latex 115, 180 nm particles on polysulfone membrane at different carrier solutions. Channel/cross flow rates are 2.2/0.7 mL/min. Each surfactant concentrations are 0.1% added with 0.02% sodium azide.

MARCEL DEKKER, INC.
270 Madison Avenue, New York, New York 10016

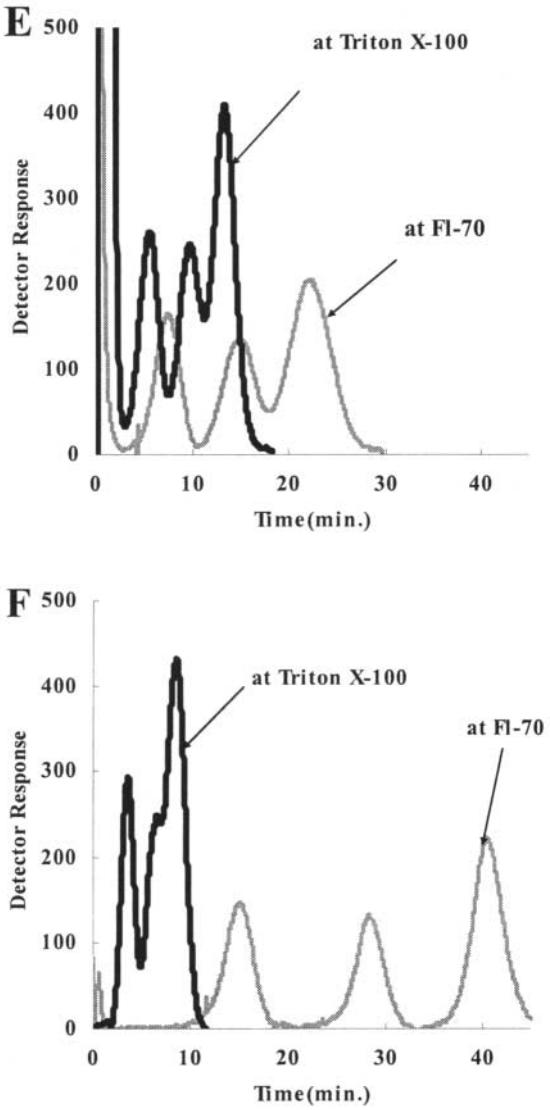

Figure 13. Fractograms of (E) polystyrene latex standards 50, 105, 152 nm particles on regenerated cellulose membrane and (F) polystyrene latex standards 50, 105, 152 nm particles on polysulfone membrane at different carrier solutions. Channel/cross flow rates are 2.2/0.7 mL/min. Each surfactant concentrations are 0.1% added with 0.02% sodium azide.

MARCEL DEKKER, INC.
270 Madison Avenue, New York, New York 10016

These surfactant molecules were easily adsorbed on the membrane surface and should change the hydrophobic surface property of the membrane. And they helped the penetration of the carrier solution through the membrane pore. Because of the slightly negative charged hydrophilic surface of the regenerated cellulose membrane, the intrinsic influence of surfactant adsorption is relatively reduced, so the departure of retention time is not so much greater than that of the polysulfone membrane. Figures 11–13 show the outstanding results between the regenerated cellulose membrane and the polysulfone membrane at different kinds of surfactant conditions.

Retention behavior of the polystyrene latex samples at the Fl-70 carrier solution agrees with the nominal size compared with that of the polysulfone membrane. The differences between Fl-70 and Triton X-100 are clearly shown in Figs. 14–17. The plot of the calculated hydrodynamic diameter shows the difference at various cross flow rates at different kinds of surfactant conditions. When the sample particles are under the external field, the equilibrium position of the sample particles are shifted toward the accumulation wall. The particles focused at the upper equilibrium position will elute earlier than those focused at the lower equilibrium position, which causes the particle cloud focused at different equilibrium positions and separated from each other to produce a double peak. These mechanisms agree with the retention behavior at the Fl-70 condition, but make it hard to apply the retention behavior at Triton X-100 condition. As the field strength increases, the lower equilibrium position shifts more toward the accumulation wall and the upper equilibrium position shifts more toward the channel center. Therefore, the separated peaks will be merged and the retention ratio of the particle will increase with an increasing flow rate. There are two interpretations to explain the retention at the Triton X-100 condition. One is the increase of the repulsion force between the membrane wall and the polystyrene latex particles at a certain distance close enough to the wall. From the basis of the DLVO theory, the repulsion force is increased near the wall. At a strong field condition, the equilibrium position of particles is close enough to the accumulation wall, and there are small hydrophilic residues on the surface of the polysulfone membrane, unlike that of the regenerated cellulose membrane.[35] The other interpretation is the increasing of the shear force at the strong cross flow rate condition. The mechanical strength of the polysulfone membrane is, in fact, more rigid than that of the regenerated cellulose membrane. The increase of field strength, increment of membrane pore size, and swelling tendency are unlike that of the regenerated cellulose membrane, it causes the upstream of cross flow near the accumulation wall. Consequently, the equilibrium positions mix with the upper position of sample materials,[36–39] so the separated peaks merged to the earlier retained peak and was shown as the single peak. It may be assumed that the equilibrium position shifts toward the channel center as the field strength increases,[40]

MARCEL DEKKER, INC.
270 Madison Avenue, New York, New York 10016

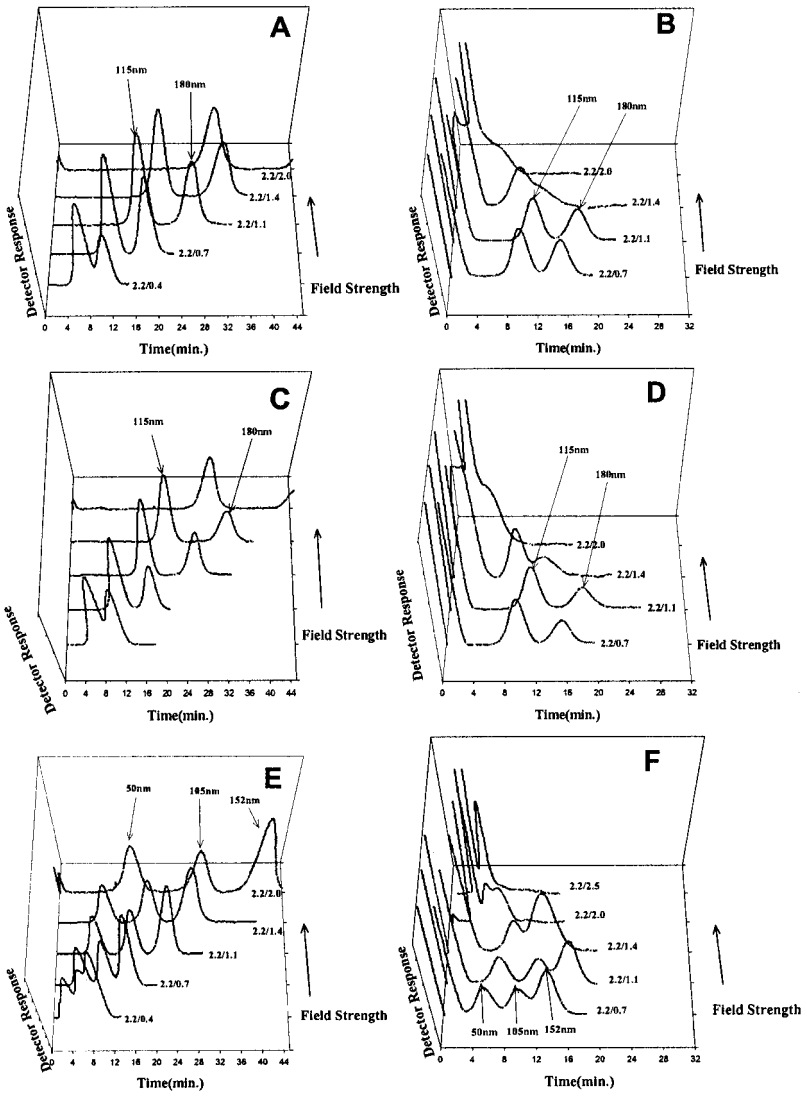

Figure 14. Fractograms of (A) high charged PS latex 115, 180 nm particles, (C) low charged PS latex 115, 180 nm particles, (E) polystyrene latex standards 50, 105, 152 nm particles at Fl-70 as carrier solution and (B) high charged PS latex 115, 180 nm particles, (D) low charged PS latex 115, 180 nm particles, (F) polystyrene latex standards 50, 105, 152 nm particles at Triton X-100 condition on regenerated cellulose membrane. Channel/cross flow rates are 2.2/0.7 mL/min. Each surfactant concentrations are 0.1% added with 0.02% sodium azide.

MARCEL DEKKER, INC.
270 Madison Avenue, New York, New York 10016

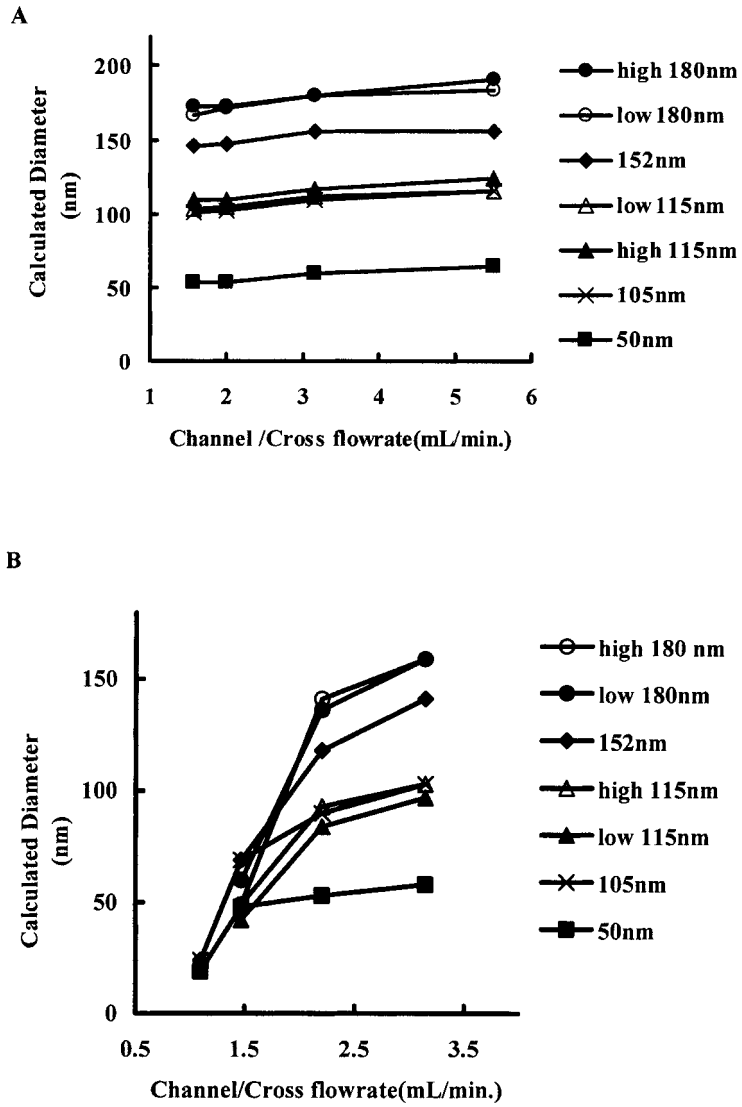

Figure 15. Calculated hydrodynamic diameter of PS latex 50, 105, 152 nm and high & low charged 115, 180 nm PS latex at Fl-70 condition (A) and Triton X-100 condition (B) at various field strengths on regenerated cellulose membrane. Carrier solution is 0.1% surfactant added with 0.02% NaN_3.

MARCEL DEKKER, INC.
270 Madison Avenue, New York, New York 10016

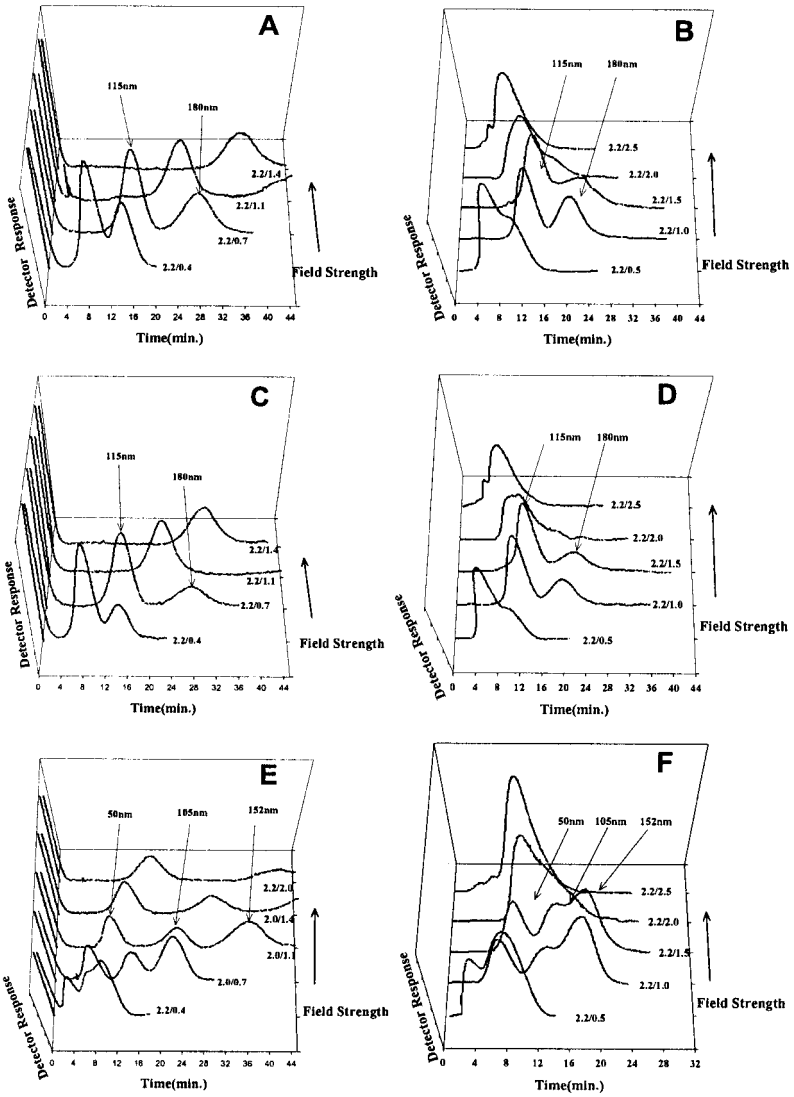

Figure 16. Fractograms of (A) high charged PS latex 115, 180 nm particles, (C) low charged PS latex 115, 180 nm particles, (E) polystyrene latex standards 50, 105, 152 nm particles at Fl-70 as carrier solution and (B) high charged PS latex 115, 180 nm particles, (D) low charged PS latex 115, 180 nm particles, (F) polystyrene latex standards 50, 105, 152 nm particles at Triton X-100 condition on polysulfone membrane. Channel/cross flow rates are 2.2/0.7 mL/min. Each surfactant concentrations are 0.1% added with 0.02% sodium azide.

MARCEL DEKKER, INC.
270 Madison Avenue, New York, New York 10016

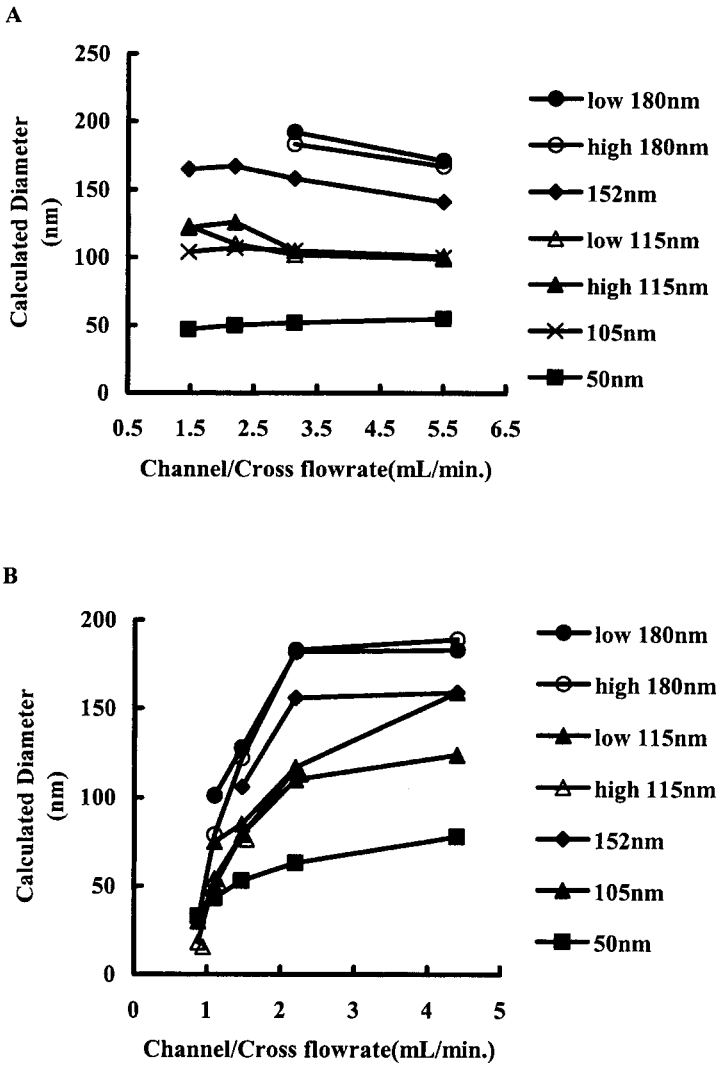

Figure 17. Calculated hydrodynamic diameter of PS latex 50, 105, 152 nm and high & low charged 115, 180 nm PS latex at Fl-70 condition (A) and Triton X-100 condition (B) at various field strengths on polysulfone membrane. Carrier solution is 0.1% surfactant added with 0.02% NaN_3.

MARCEL DEKKER, INC.
270 Madison Avenue, New York, New York 10016

therefore, the retention time will decrease by increasing the cross flow rate at the Triton X-100 condition.

In addition, the focusing condition of the sample cloud may be altered during the relaxation time. These alterations are also caused by the difference of hydrophobicity of the accumulation wall.[41–43] In fact, the degree of

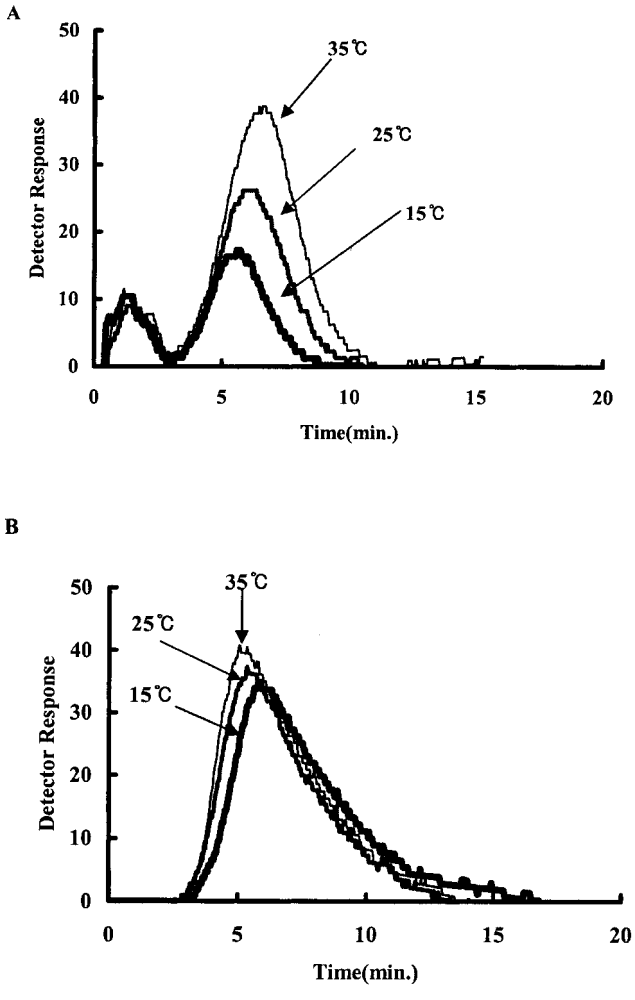

Figure 18. Fractograms of Au 20 nm colloid at different temperature conditions on regenerated cellulose membrane (A) and on polysulfone membrane (B). Channel/cross flow rates are 1.0/2.2 mL/min. Carrier solution is 0.05% CTAB added with 0.02% sodium azide.

MARCEL DEKKER, INC.
270 Madison Avenue, New York, New York 10016

swelling is mainly affected by the thickness of the electronic double layer between the polysulfone membrane and the sample cloud.

Retention of Nano-Sized Gold Colloid

We also studied the retention behavior of smaller particles such as the nano-sized gold colloid. Nano-sized gold colloids are useful materials in many areas of semiconductor manufacturing. Because of its higher surface area to volume ratio, electronic properties differ from those of bulk materials. Such a quantum confinement effect is important for advanced techniques in many areas of semiconductor manufacturing. Moreover, the separation techniques of each nano-sized particle is rapidly becoming important for a range of application. In this work, 5, 10, and 20 nm-sized gold colloid standards were separated at appropriate dispersion conditions and we calculated the particle size distribution by the FlFFF system. Retention behavior of probe molecules also could indicate the information of membrane surface properties. A 20 nm-sized gold colloid is used for probe molecules on two different membranes, at several temperature conditions. Recovery of 20 nm gold colloids is increased on the regenerated cellulose membrane by increments of system temperature, but there is no significant change on the polysulfone membrane. Figure 18 shows the fractograms of 20 nm sized gold colloidal particles at different

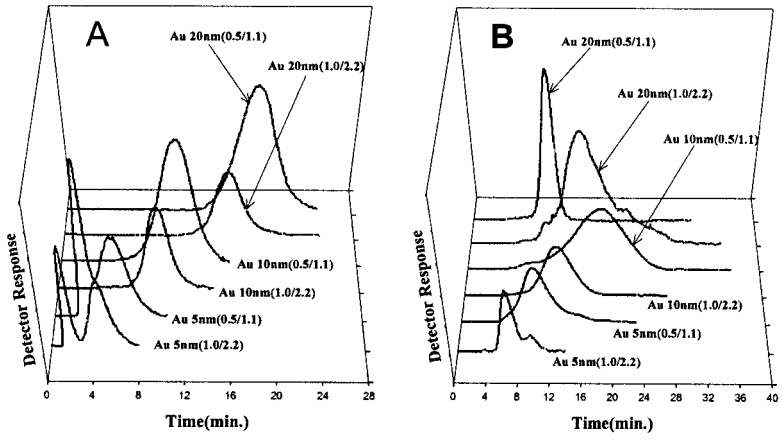

Figure 19. Fractograms of Au 5, 10, 20 nm colloids at Fl-70 conditions (A) and Triton X-100 conditions (B) on regenerated cellulose membrane. Channel/cross flow rates are 1.0/2.2 mL/min and 0.5/1.1 mL/min. Carrier solution is 0.1% surfactant added with 0.02% sodium azide at 25°C.

MARCEL DEKKER, INC.
270 Madison Avenue, New York, New York 10016

temperature on two different membranes. These results indicate that the physical surface morphology of the regenerated cellulose membrane is more flexible than that of the polysulfone membrane. Comparison of the retention behavior of the different surfactant conditions like polystyrene latex particles and retention time of 20 nm-sized gold colloid particles were reversed at the

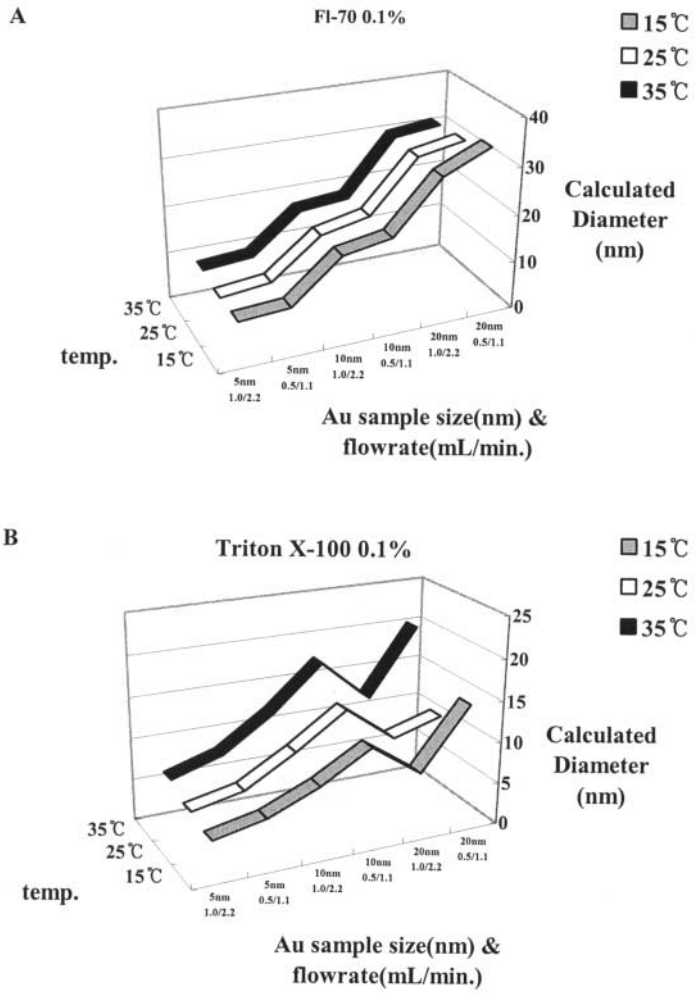

Figure 20. Calculated hydrodynamic diameters of Au 5, 10, 20 nm colloids at Fl-70 conditions (A) and at Triton X-100 conditions (B) on regenerated cellulose membrane. Channel/cross flow rates are 1.0/2.2 mL/min, 0.5/1.1 mL/min.

MARCEL DEKKER, INC.
270 Madison Avenue, New York, New York 10016

Triton X-100 condition. These results indicate that the particle–wall interaction is greatly affected by the membrane swelling property, even if using nano-sized particles. Figure 19(B) shows the early elution tendency of 20 nm sized gold colloidal particles at Triton X-100 condition. At a certain field strength, the equilibrium layer of larger sized particles (20 nm Au colloid) approached the membrane surface more than that of smaller ones (5, 10 nm Au colloid), so the retention time of the 20 nm-sized gold colloid was dramatically influenced by the hydrodynamic lift force near the channel wall. Retention behavior of 5, 10, 20 nm sized gold colloidal particles are shown in Fig. 20.

CONCLUSION

The electrostatic and van der Waals particle–wall interactions have an important role in departure from the ideal relationship. This departure in particle size analysis may cause significant error in practical application. In this work, investigation of retention perturbation are measured on different types of membranes and compared with the calculated and theoretical size. Then, the appropriate conditions for each sample were chosen that minimized the perturbation. The main difference of the two applied membranes can be easily understood through a comparison with the resolution of retention peaks. As a matter of fact, several considerable points remained, such as how each carrier solution affected the swelling and wetting of the membrane polymer. The retention of particulate materials on stiff and inflexible polymer such as polysulfone membrane, which looks like it is unaffected by the carrier solution, was significantly disturbed, unlike that of the hydrophilic regenerated cellulose membrane. So, we can conclude that the retention behavior of particulate materials was mainly affected not by the intrinsic physical property of the membrane polymer, but by the wetting and penetration property, which was determined by the surfactant we used for the carrier solution. Moreover, during relaxation time, the influence of cross flow varies at different types of surfactant conditions that caused the distortion of the parabolic flow profile. The aggregation and adsorption interaction between the channel wall and the samples can be reduced effectively by adding the proper surfactant.

REFERENCES

1. Mulder, M. In *Basic Principles of Membrane Technology*, 2nd Ed.; Kluwer Academic Publishers, 1996; Chap. 2, 56–59.

MARCEL DEKKER, INC.
270 Madison Avenue, New York, New York 10016

2. Howell, J.A.; Sanchez, V.; Field, R.W. Nature of membranes. In *Membranes in Bioprocessing Theory and Application*, 1st Ed.; Chapman & Hall, 1993; Chap. 2, 32–47.
3. Osada, Y.; Nakagawa. Microfiltration and ultrafiltration. In *Membrane Science and Technology*; Marcel Dekker, Inc., 1992; Chap. 8, 289–335.
4. Giddings, J.C. Science **1993**, *260*, 1456–1465.
5. Giddings, J.C. Anal. Chem. **1995**, *67*, 592A–598A.
6. Hartmann, R.L.; Williams, S.K.R. J. Membrane Sci. **2002**, *209*, 93–106.
7. Williams, P.S.; Xu, Y.; Reschiglian, P.; Giddings, J.C. Anal. Chem. **1997**, *69*, 349–360.
8. Jensen, K.D.; Williams, K.R.; Giddings, J.C. J. Chromatography A **1996**, *746*, 137–145.
9. Yau, W.W.; Kirkland, J.J. Anal. Chem. **1984**, *56*, 1461–1466.
10. Williams, P.S.; Moon, M.H.; Giddings, J.C. Coll. Surf. Physicochem. Engn. Aspects **1996**, *113*, 215–228.
11. Giddings, J.C. In *Unified Separation Science*; John Wiley & Sons, Inc., 1991; Chap. 9, 213–214.
12. Cheong, I.W.; Kim, J.H. Colloid Polym. Sci. **1997**, *275*, 736.
13. Kim, J.H.; Chainey, M.; Elaasser, M.S.; Vanderhoff, J.W. J. Poly. Sci. A: Poly. Chem. **1989**, *27*, 3189.
14. Yoon, J.Y.; Park, H.Y.; Kim, J.H.; Kim, W.S. J. Coll. Interface Sci. **1996**, *177*, 618.
15. Mori, Y.; Kimura, K.; Tanigaki, M. Anal. Chem. **1990**, *62*, 2668–2672.
16. Prieve, D.C.; Hoysan, P.M. J. Coll. Interf. Sci. **1978**, *64*, 201.
17. Koliadima, A.; Karasikakis, G. J. Chromatogr. **1990**, *517*, 345.
18. Karasikakis, G.; Athanasopoulou, A.; Koliadima, A. J. Microcol. Sepn. **1997**, *9* (4), 275.
19. Athanasopoulou, A.; Karasikakis, G.; Travlos, A. J. Liq. Chromatogr. & Rel. Technol. **1997**, *20* (16 & 17), 2525.
20. Koliadima, A.; Gravril, D.; Karasikakis, G. J. Liq. Chromatogr. & Rel. Technol. **1999**, *22* (18), 2779.
21. Karasikakis, G.; Koliadima, A.; Farmakis, L.; Gravril, D. J. Liq. Chromatogr. & Rel. Technol. **2002**, *25* (13–15), 2153.
22. Hansen, M.E.; Giddings, J.C. Anal. Chem. **1989**, *61*, 811–819.
23. Visser, J. Adv. Coll. Interf. Sci. **1972**, *3*, 331.
24. Schrader, M.E.; Leob, G.I. High- and medium-energy surfaces: ultra high vacuum approach. In *Modern Approaches to Wettability*; Plenum Press: New York, 1992; Chap. 3, 61 pp.
25. Ahmadi, G. In *Clarkson University web site lecture note*; http://www.clarkson.edu/projects/fluidflow/courses/me537/5_vanderWaals.pdf
26. Parsegian, V.A.; Weiss, G.H. J. Coll. Interf. Sci. **1981**, *81*, 285.
27. Zauscher, S.; Klingenberg, D.J. J. Coll. Interf. Sci. **2000**, *229*, 497–510.

MARCEL DEKKER, INC.
270 Madison Avenue, New York, New York 10016

28. Benavente, J.; Jonsson, G. Coll. Surface A: Physicochem. Surf. Engn. Aspects **1998**, *138*, 255–264.
29. Yuan, W.; Zydney, A.L. Environ. Sci. Technol. **2000**, *34*, 5043–5050.
30. Benincasa, M.A.; Giddings, J.C. Anal. Chem. **1992**, *64*, 790–798.
31. Tsujii, K. In *Surface Activity: Principles, Phenomena, and Application*; Academic Press, 1998; Chap. 8, 17–42.
32. Kalchevsky, P.A.; Danov, K.D.; Denkov, N.D. Chemical physics of colloid systems and interfaces. In *Handbook of Surface and Colloid Chemistry*; Birdi, K.S., Ed.; CRC, LLC., 1997; Chap. 11, 430 pp.
33. Toshihiko, J.; Higa, M.; Minoura, N.; Tanioka, A. Macromolecules **1998**, *31*, 1277–1284.
34. Wittgren, B.; Wahlund, K.G.; Derand, H.; Wesslen, B. Macromolecules **1996**, *29*, 268–276.
35. Gancarz, J.; Pozniak, G.; Bryjak, M.; Frankiewicz, A. Acta Polym. **1999**, *50*, 317–326.
36. Cheryan, M. In *Ultrafiltration and Microfiltration Handbook*; Technomic Publishing Co., Inc., 1998; 127–161.
37. Beckett, R.; Giddings, J.C. J. Coll. Inter. Sci. **1997**, *186*, 53–59.
38. Lee, Y.; Clark, M.M. J. Membrane Sci. **1998**, *149*, 181–202.
39. Li, H.; Fane, A.G.; Coster, H.G.L.; Vigneswaran, S. J. Membrane Sci. **2000**, *172*, 135–147.
40. Hansen, M.E.; Giddings, J.C. J. Coll. Interf. Sci. **1988**, *132* (11), 300–312.
41. Williams, P.S.; Koch, T.; Giddings, J.C. Chem. Eng. Comm. **1992**, *111*, 121–147.
42. Williams, P.S.; Lee, S.; Giddings, J.C. Chem. Eng. Comm. **1994**, *130*, 143–166.
43. Kim, C.K.; Kim, S.S.; Kim, D.W.; Lim, J.C.; Kim, J.J. J. Membrane Sci. **1998**, *147*, 13–22.

Received April 9, 2003
Accepted June 10, 2003
Manuscript 6035

MARCEL DEKKER, INC.
270 Madison Avenue, New York, New York 10016

MARCEL DEKKER, INC.
270 Madison Avenue, New York, New York 10016